2012 12th IEEE-RAS International Conference on Humanoid Robots
Nov.29-Dec.1, 2012. Business Innovation Center Osaka, Japan

Evaluation of a Stabilizer for Biped Walk with Toe Support Phase

Shuuji Kajita*, Kanako Miura, Mitsuharu Morisawa, Kenji Kaneko, Fumio Kanehiro* and Kazuhito Yokoi
Humanoid Robotics Group, Intelligent systems institute, AIST, Tsukuba, Ibaraki, 305-8568, Japan
Email: s.kajita@aist.go.jp
* Japan Science and Technology Agency, CREST

***Abstract*—We discuss a feedback controller to stabilize biped walking which has toe support phase mimicking human gait. Using a reference walking pattern proposed in our previous work [11], our stabilizer can realize reliable walking. To evaluate the quality of stabilization, we propose two indicators, the maximum floor reaction force and the root mean square of the CoM tracking error. From our walking experiments, these indicators suggest us two policies of control parameter tuning, (1) not to control ZMP at toe support, and (2) not to use the ZMP phase-lead compensation for sagittal motion. These findings were validated by simulations of linear inverted pendulum model. It is shown that the observed behavior of the controller is caused by large velocity dissipation at support exchange.**

I. Introduction

Toe joints are beneficial for a biped walking robot in many aspects. In the pioneering work of Nishiwaki et al., it was demonstrated that toe joints can (1) increase walking speed, (2) help go up higher step, and (3) help whole-body action at knee contact state [1]. Ogura et al. realized biped walk with big step length up to 50cm by WABIAN-2R equipped with passive toe joints [5]. Buschmann et al. developed biped robot LOLA with active toe joints, which can perform fast walk up to 3km/h [2], [3]. Tajima et al. developed a running biped with active toe joints, which can run at 7km/h.

Some of above mentioned works have already achieved good stability. For example, Tajima's robot can handle big external disturbance during its running. However, their control partially relies on the large toe supporting area. We believe a stabilization control for walking with toe support is important, especially when the toes are passive and/or small. One contribution toward this direction was done by Hashimoto et al. who proposed an energy based control strategy for WABIAN-2R with passive toe [7].

This paper discusses a walking control of our biped humanoid robot HRP-4C (Fig.1). It is a humanoid robot of 160cm height, 48kg weight and total 44 degrees of freedom (DOF) [8]. Since our robot was designed to have close dimensions of the average Japanese young female, its toes are small compared with conventional biped robots. On the other hand, the toes are driven by servomotors, which is different from the passive toes used in WABIAN-2R.

Using HRP-4C, Miura et al. have realized a human-like walking which was designed to have toe support phase before the heel contact and to have a knee as stretched as possible

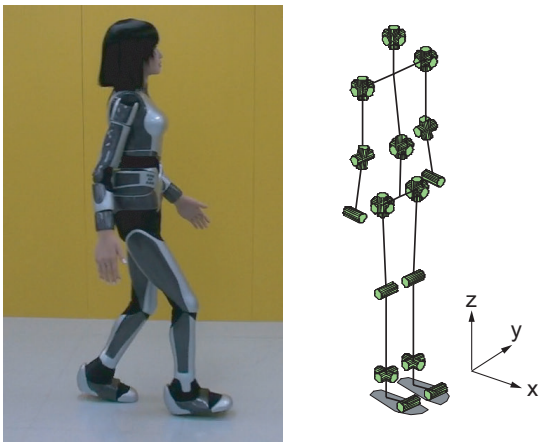

Fig. 1. Left: Walking cybernetic human HRP-4C at toe support phase. Right: joint configuration (face control joints and hands are omitted)

[11]. The same walking pattern is used in this report, but we discuss the control issues in more detail.

In this paper, we evaluate the quality of the stabilization, which is affected by many tunable parameters of our stabilizer. When it is poorly tuned, a robot can easily fall down even on a flat floor without any external disturbance. Until now, these parameters were tuned by trial and error. To obtain a good performance of stabilizer, we have tested many walk experiments with different parameter setting, which took a few days in some case. Therefore, it is necessary to establish a systematic way of parameter tuning as well as a quantitative measures for the quality of stabilization.

The rest part of this paper is organized as follows. In Section II, we explain a stabilizer to handle toe support phase. In Section III, a typical experimental result is shown and we propose two indicators to measure the quality of walk control. Using these indicators, we seek better tuning of foot torque controller (Section IV) and ZMP phase-lead compensator (Section V). In Section VI, we discuss the implications of the result and conclude this report.

II. Stabilizer for walking with toe support phase

A. Base frame for CoM/ZMP measurement

For a biped walking robot, the center of mass (CoM) and the Zero-Moment Point (ZMP) are the fundamental physical

properties [9]. To measure them, we used a frame placed on the supporting sole in our previous report [10]. However, this gives us a wrong measurement when a robot walks using toes, since the sole rotates around the toe joint and it is no longer an inertial frame.

Figure 2 illustrates an improved setting of base frame Σ_{base} to measure the CoM and ZMP for each support phase. Its origin is placed on the floor surface at fixed distance from the supporting toe joint. The x,y axis of the base frame are aligned to the horizontal toe orientation and the z axis is set vertical based on the inertial measurement unit (IMU) equipped on the body.

We have offset the origin of the base frame from the supporting toe, because our former stabilizer used the base frame on the sole just below the supporting ankle. When our new controller takes a walking pattern without toe bending, this definition of Σ_{base} provides the identical CoM and ZMP to the previous one.

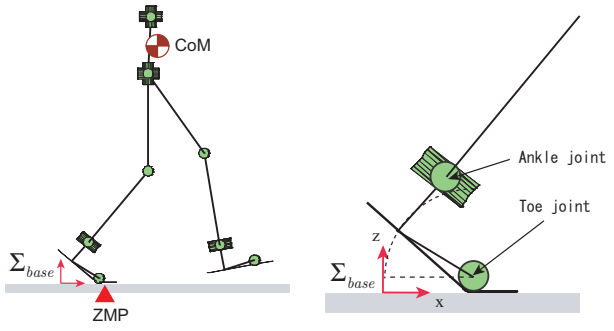

(a) Base frame for measurement (b) Base frame setting

Fig. 2. Base frame for measurement

B. Robot dynamics with ZMP control delay

A walking robot dynamics can be approximated by the following equation both in the sagittal plane and in the lateral plane [12].

$$\ddot{x} = \frac{g}{z_c}(x - p) \tag{1}$$

where x is the horizontal position of the CoM, z_c is CoM height, and g is gravity acceleration. We regard the ZMP p as a state variable whose dynamics is determined by the following equation.

$$p = \frac{1}{1 + sT_p^*}p^d \tag{2}$$

where T_p^* is the time constant of the ZMP controller and p^d is the desired ZMP. The validity of this model was confirmed in our former report [10].

C. CoM tracking control with ZMP phase-lead filter

Let us define the state vector of the system as $\boldsymbol{x} := [x,\ \dot{x},\ p]^T$. A walking pattern generator creates a reference state $\boldsymbol{x}^{pg} := [x^{pg},\ \dot{x}^{pg},\ p^{pg}]^T$ which satisfies (1), such that

$$\ddot{x}^{pg} = \frac{g}{z_c}(x^{pg} - p^{pg}). \tag{3}$$

Then, we can regard a stabilizer as a tracking controller to let the state error $\boldsymbol{x} - \boldsymbol{x}^{pg}$ to be zero. It is done by giving the desired ZMP as follows.

$$p^d = (1 + sT_p)p^{pg} + \Delta p, \tag{4}$$

where Δp is the ZMP modification for the stabilization given by

$$\Delta p = k_x(x^{pg} - x) + k_v(\dot{x}^{pg} - \dot{x}) + k_p(p^{pg} - p). \tag{5}$$

The state feedback gains k_x, k_v, k_p are calculated by pole assignment. In this report, we specified the poles as $(-20, -3.5, -\omega)$ where $\omega := \sqrt{g/z_c}$. To obtain the maximum stability, one of the poles is set to match the eigen value of the original inverted pendulum [13].

The filter $(1+sT_p)$ in (4) is a ZMP phase-lead compensator to achieve accurate CoM tracking. In an ideal case, we should choose $T_p = T_p^*$ to cancel the ZMP delay, we however tune it as a control parameter in Section V. Note that $(1+sT_p)$ is a non-proper function prohibited in standard control theory. Nevertheless, it can be implemented as an almost equivalent filter in discrete time domain.

Figure 3 illustrates the overall structure of our stabilizer with the ZMP phase-lead compensation. To stabilize HRP-4C walking in 3D space, two independent controllers are used for sagittal and lateral motion.

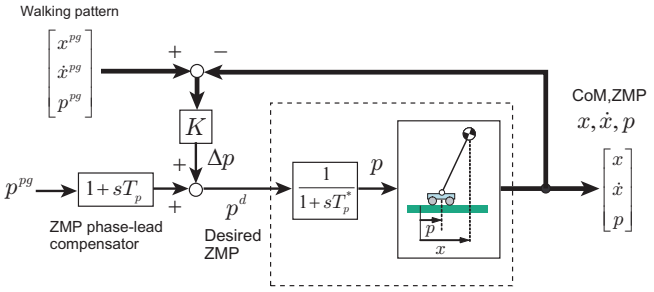

Fig. 3. Tracking controller with inverse system

D. Torque controller implementation

The desired ZMP (4) is converted into torque references. For example, sagittal component of desired ZMP p^d is converted into the desired pitch torque of supporting foot τ^d.

To realize the desired foot torque τ^d, we calculate a "torque control angle" δ by the following damping (impedance) controller.

$$\begin{aligned} \delta^\star &= \int \{D^{-1}(\tau^d - \tau) - \frac{1}{T}\delta\}dt, \\ \delta &= sat(\delta^\star, \delta_{max}) \end{aligned} \tag{6}$$

where D is damping gain. T is a time constant to retrieve the neutral point when the foot is in the air at swing phase.

We used a saturation function $sat()$ to limit the control angle within the specified range δ_{max}.

$$sat(\delta^\star, \delta_{max}) := \begin{cases} \delta_{max} & \text{if } \delta^\star > \delta_{max} \\ \delta^\star & \text{if } |\delta^\star| \leq \delta_{max} \\ -\delta_{max} & \text{if } \delta^\star < -\delta_{max} \end{cases} \quad (7)$$

Finally the torque control angle δ are added to the given walking pattern as

$$q^d = q^{pg} + \delta, \quad (8)$$

where q^{pg} is the joint angle of the walking pattern and q^d is the reference for the joint servo controller.

III. Experimental results

With the proposed stabilizer and the given walking pattern, our robot can perform reliable biped walking with big strides. In this section, we first present a typical result of the experiment, and then we introduce performance indicators to evaluate the quality of a walk control. These indicators are used to tune the control parameters in the following sections.

A. Reference walking pattern

We generated a walking pattern whose steps are specified as Table I by the algorithm discussed by Miura et al. [11]. Its total travel distance is 2.8m and the steady walking speed is 1.8km/h in the middle of the walking.

TABLE I
Step length, Single and Double support periods

step no.	support leg	length[m]	SS [s]	DS [s]
1	Right	0.25	0.7	0.1
2	Left	0.35	0.7	0.1
3-6	Right/Left	0.40	0.7	0.1
7	Right	0.35	0.7	0.1
8	Left	0.25	0.7	–

The floor projections of the CoM and ZMP of walking pattern and the corresponding experimental result are shown in Fig. 4.

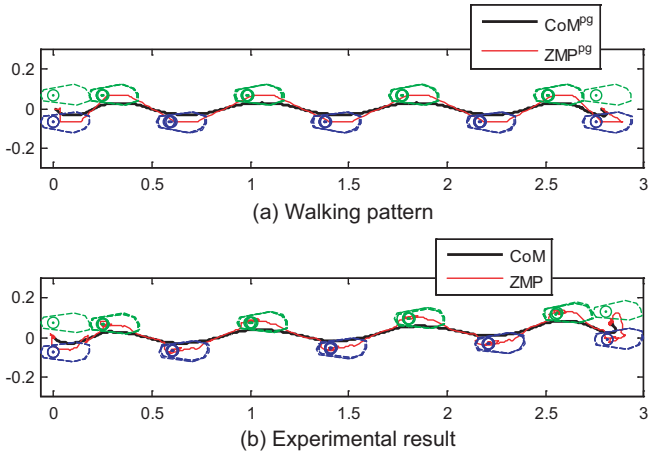

Fig. 4. Walking pattern and experimental result in top view

B. CoM tracking

Figure 5 shows the time profile of CoM and ZMP for the first four steps of our walking experiment. In the upper graph the sagittal CoM and pattern CoM are plotted by bold black line and thin blue line, respectively. They are measured with respect to the base frame defined at each support (see Fig.2).

The vertical dotted lines indicate the change of support phase between double support (DS) periods and single support (SS) periods. During single support, the pattern ZMP (thin magenta line) moves from the origin to the toe region (yellow area) to guarantee the support by the toe link. The ZMP is shown by the bold red line. At the end of each single support phase (SS), it reaches the toe region which represents that the robot goes into toe support phase.

The lower graph of Fig.5 shows the lateral CoM, ZMP and their references. Compared with the sagittal control, we see better CoM tracking.

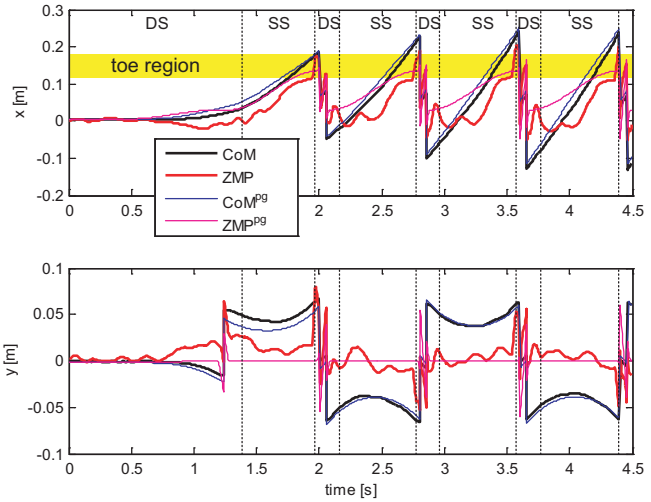

Fig. 5. CoM and ZMP. DS:Double support, SS:Single support

To evaluate the CoM tracking in sagittal and lateral direction, we define indicators which are root mean squares of the tracking errors.

$$I_x = \sqrt{\frac{1}{T_{pg}} \int_0^{T_{pg}} (x(t) - x^{pg}(t))^2 dt} \quad (9)$$

$$I_y = \sqrt{\frac{1}{T_{pg}} \int_0^{T_{pg}} (y(t) - y^{pg}(t))^2 dt}, \quad (10)$$

where T_{pg} is the length of the walking pattern.

C. Floor reaction force

Figure 6 shows the vertical floor reaction forces of the first four steps. From the second support phase which starts around 2s, we can observe double peak profile which is characteristic in human biped locomotion.

When our robot walks under a poor stabilizing control, we observe high peaks of f_z due to body vibration and undesired touchdowns. This can be used as another indicator of walking

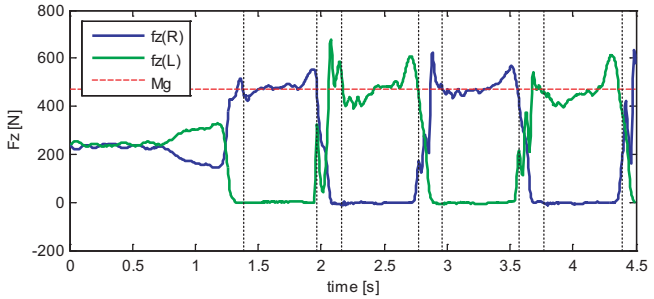

Fig. 6. Floor reaction forces

control. We have decided to use F_{max}, the highest peak of the floor reaction force.

$$F_{max} = \max_{t\in[0,T_{pg}]} \max(f_{Rz}(t), f_{Lz}(t)) \qquad (11)$$

Alternatively, it is possible to use standard deviation or power of high pass filtered force signal. Nevertheless, we preferred to use a peak of the original sensor signal, because its physical meaning is clear. A walking robot must take care of the maximum impulsive force for it is the main threat to the hardware.

IV. Foot Torque Controller Tuning

A. Experimental result of torque control

Figure 7(a) shows the foot torques in our walking experiment. The bold lines are pitch torques of right and left foot and the thin lines are the desired values. The foot torques were measured by the force sensors equipped in the ankles and shown in the base frame Σ_{base}. Since the ZMP moves from heel to toe in each single support phase, the target foot torque decrease until it reaches the minimum value which corresponds to the toe supporting. It returns to zero when the foot starts to swing.

The torque control angles are shown in Fig.7(b). It saturated by the specified value ($\delta_{max} = 5$deg, see Section II-D). The saturation occurred at each latter half of single support, which approximately corresponds to toe supporting periods. This means the foot pitch torque was not controlled during toe support. Indeed, we can observe the torque (bold line) did not track the desired value as shown by the arrow in Fig.7(a).

B. Effect of torque control angle saturation

We conducted walking experiments with different torque control angle limits δ_{max} for pitch torque. To compare the results, the root mean square of CoM tracking errors I_x, I_y and the maximum floor reaction force F_{max} are plotted in Fig.8.

For a very small angle limit $\delta_{max} = 3$deg, the robot could not walk. we can confirm this in Fig.8 by huge tracking errors and huge maximum floor reaction force 1200N, which is almost three times of the robot weight. This is because the

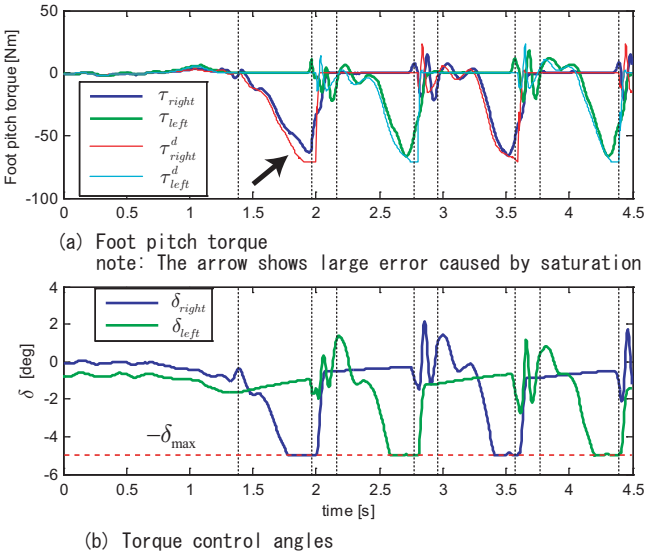

Fig. 7. Foot torques

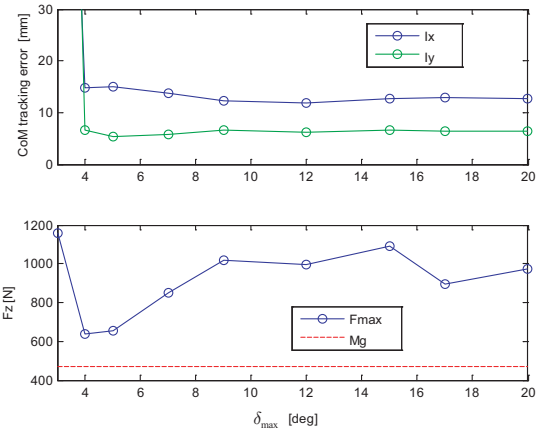

Fig. 8. Effect of torque control angle limit $\delta_{max} = 3 \sim 20$mm

ankle pitch torque was not controlled well by the lack of sufficient control input.

When the torque control angle limits are larger than 4deg the robot could walk, but the quality of walking apparently changes depending on its value. When we watch the tracking error I_x (blue line in the upper graph of Fig.8), it slightly decrease by the growth of δ_{max}. This makes sense since larger δ_{max} can realize more accurate foot pitch torque which helps the CoM control in x direction.

On the other hand, we observe the smallest maximum floor reaction force is realized at $\delta_{max} = 4$deg, and it increases by larger angle limits. That means the smoothest walk is realized by a limited foot torque control with saturation (see Fig.7).

This can be explained by the occurrence of foot rotation around the toe edge. When ZMP is controlled close to the support polygon edge, the toe link eventually looses the full contact with the ground. This may introduce the up/down

motion of CoM which was not planned by the walking pattern. Thus it results the fluctuation of the ground reaction force.

The foot rotation around the toe edge can be confirmed by Fig. 9(a), which plots the absolute posture of the toe link. With large torque control angle limit, they increase toward the end of each support phase (pointed by arrows) although they should remain zero. Meanwhile they are kept almost horizontal by using small δ_{max} as seen in Fig. 9(b). The small inclination of few degrees at the end of support phase is caused by the mechanical compliance of the robot feet.

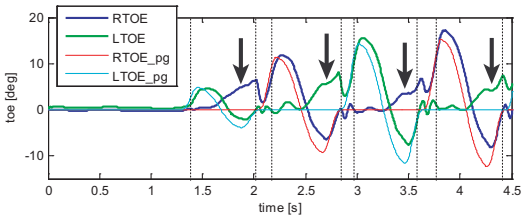

(a) The supporting toe links rotate at $\delta_{\max} = 12\text{deg}$

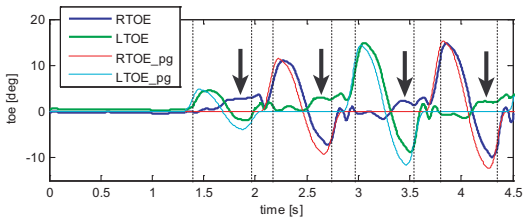

(b) The supporting toe links are kept horizontal at $\delta_{\max} = 4\text{deg}$

Fig. 9. Toe link posture

V. Effect of ZMP phase-lead compensation

A. Experiment

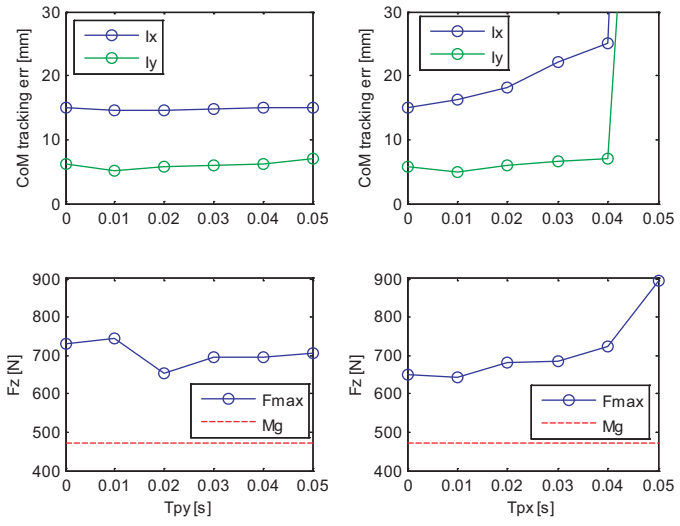

(a) Lateral compensation ($T_{px} = 0\text{s}, T_{py} = 0 \sim 0.05\text{s}$)

(b) Sagittal compensation ($T_{px} = 0 \sim 0.05\text{s}, T_{py} = 0.02\text{s}$)

Fig. 10. Effect of the ZMP phase-lead compensation

We conducted walking experiments with different ZMP phase-lead compensation settings. To explain our experiments, we introduce new symbols T_{px} and T_{py} for the ZMP phase-lead compensators in sagittal and lateral directions, respectively.

In the first set of experiments, we changed the lateral compensator T_{py} while keeping the sagittal one as $T_{px} = 0\text{s}$. The results are shown in Fig.10(a), which indicates that $T_{py} = 0.02\text{s}$ gives the smoothest walk in terms of the maximum floor reaction force observed in the lower graph.

In the second set of experiments, we changed the sagittal compensator T_{px} while keeping the lateral one as $T_{py} = 0.02\text{s}$. The results are shown in Fig.10(b). We observe that the increase of T_{px} degenerates the CoM tracking control quality (error increased) as well as it harms the walking smoothness (maximum floor reaction force increased). This result tells us the ZMP phase-lead compensation is no use for the sagittal CoM tracking control, and we should use $T_{px} = 0\text{s}$ for our stabilization.

B. Simulation with heel strike dissipation

To understand this unexpected result, let us watch the experimental result carefully. Figure 11 shows CoM and ZMP control using the ZMP phase-lead compensations of $T_{px} = 0.04\text{s}$. In the upper graph, we can observe big error between the reference (thin blue line) and the real CoM (bold black line) same as indicated in Fig.10(b).

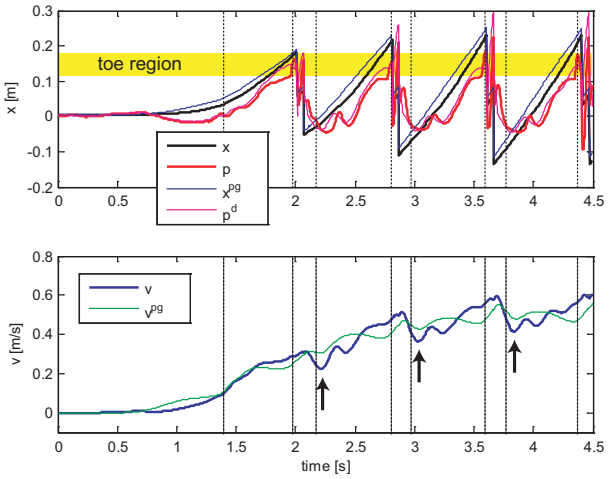

Fig. 11. CoM tracking position and velocity ($T_{px} = 0.04$)

The lower graph of Fig.11 shows the CoM velocity (bold line) and its reference (thin line). It is remarkable that the CoM velocity largely drops after double support periods (shown by arrows) while the reference does not have such profile.

This observation reminds us dissipation at heel strike, which is considered in limit cycle walkers [14]. Although most of the ZMP-based walking robots have not been taking into account of such dissipation, it exists in reality!

Note that, the CoM speed drops in the middle of the double support phase in Fig.11. We can explain this by checking the floor reaction force data of Fig.6. Our controller detects the start of double support phase by the first faint impact of touchdown. However, the biggest impact occurs in the middle of double support phase, which may correspond to the heel strikes of passive dynamic walkers.

To see the effect of velocity dissipation, we simulated a CoM tracking control. We used ZMP delayed linear inverted pendulum model (1),(2) with $T_p^* = 0.04$s and $z_c = 0.8$m. The instantaneous velocity change at each heel strike was given by

$$v^+ = dv^-, \tag{12}$$

where v^- is CoM speed before heel strike, v^+ is after heel strike, and d specifies the amount of dissipation.

Figure 12 shows the simulation result using dissipation parameter $d = 0.7$ and ZMP phase-lead compensation of $T_{px} = 0.04$s. At the second support phase which starts from 2.4s in the upper graph, there exists visible tracking error between CoM (bold black line) and its reference (thin blue line). The velocity tracking is shown in the lower graph. The arrows indicate velocity dissipation at heel strike (touchdown). The tracking error between CoM velocity (bold blue line) and its reference (thin green line) is big.

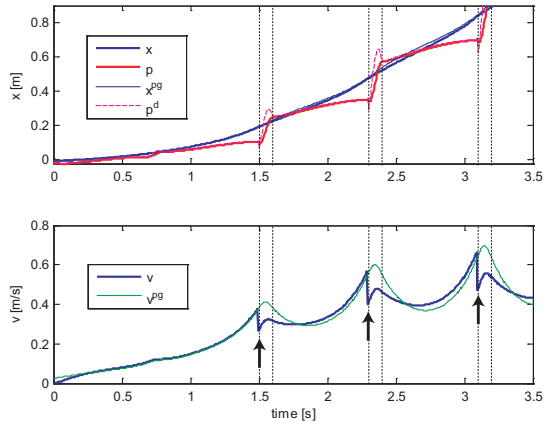

Fig. 12. Simulated CoM tracking with dissipation ($d = 0.7, T_{px} = 0.04$)

Figure 13 is the result without ZMP phase-lead compensation ($T_{px} = 0$s) using the same dissipation parameter d. The tracking of CoM position and velocity is much better than Fig.12, which coincides with the experimental result shown in the former subsection.

We simulated CoM tracking under the different ZMP phase-lead compensation and different ratio of dissipation. The change of the tracking performance is shown in Fig.14. If a robot walks with no velocity dissipation ($d = 1.0$), we get the smallest tracking error with $T_{px} = 0.05$s which is close to the ZMP delay of the system shown as the vertical broken line. Since our phase-lead compensation is not exact inverse system, the best point differs from the value of ZMP delay ($T_p^* = 0.04$s).

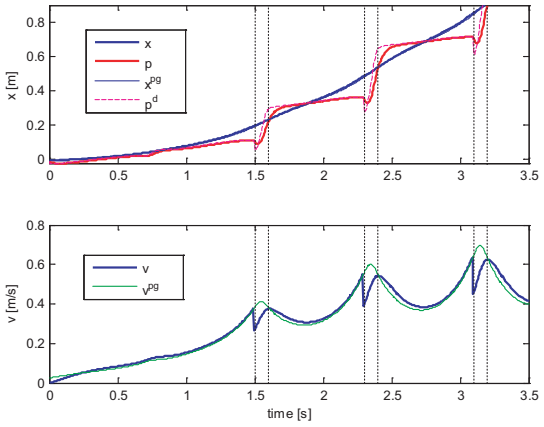

Fig. 13. Simulated CoM tracking with dissipation ($d = 0.7, T_{px} = 0.0$)

When velocity dissipation becomes severe ($d = 0.9 \rightarrow 0.6$), the best tracking point moves to zero. At $d = 0.6$, which means 40% of CoM velocity is lost at every heel strikes, ZMP phase-lead compensation of $T_{px} = 0$ gives the best performance. In this case, larger compensation always leads poorer CoM tracking, thus it explains the experimental result of Fig.10(b) in the previous subsection.

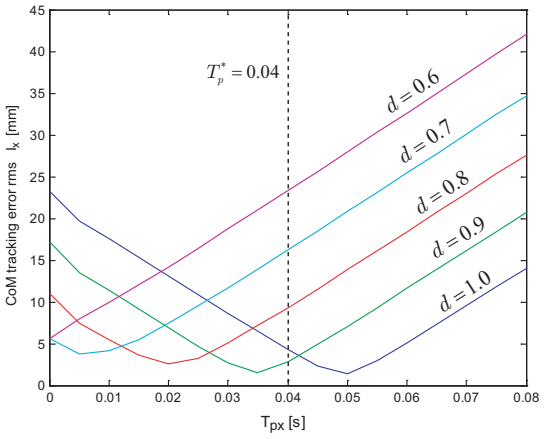

Fig. 14. CoM tracking error and ZMP phase-lead compensation

VI. Conclusion

In this paper, we conducted experiments to evaluate a feedback controller for biped walking which has toe support phase. Using the controller based on CoM/ZMP state feedback [10] and the reference walking pattern proposed in our previous work [11], our robot could perform reliable walking of 0.4m step length and 0.8s step cycle.

To evaluate the quality of stabilization, we have proposed two indicators, the maximum floor reaction force and the root mean square of the CoM tracking error. These indicators suggested us two policies of control parameter tuning, (1) not to control ZMP at toe support, and (2) not to use the ZMP phase-lead compensation for sagittal motion. These findings

were validated by simulations of linear inverted pendulum model. It was shown that our controller similarly behaves when each support exchange has large velocity dissipation.

We believe our result bridges two different biped research communities, ZMP users and limit cycle users. By introducing the period where ZMP control is not applied, our robot already can be said to be a semi-passive walker. On the other hand, we are still using precise ZMP feedback for the rest part of control, which is important for robust walk with good repeatability.

The finding that the ZMP phase-lead compensation does not work at large dissipation, is now forcing us a reconsideration of feedback controller design. On the other hand, heel strike dissipation is well acknowledged as the source of stability in the limit cycle community. ZMP people should not neglect this fact any more to realize better biped walking in speed and efficiency.

ACKNOWLEDGMENT

We thank members of humanoid robotics group, Dr. Nakaoka, Dr. Kita, Dr. Asano and Dr. Asoh for their technical help and the fruitful discussion with them. We also thank Mr.Ishiwata who developed ART-Linux 2.6, a dependable real-time operating system.

REFERENCES

[1] K.Nishiwaki, S.Kagami, Y.Kuniyoshi, M.Inaba, and H.Inoue, "Toe Joints that Enhance Bipedal and Fullbody Motion of Humanoid Robots," Proc. of IEEE Int. Conference on Robotics and Automation, pp.3105-3110, 2002.

[2] T.Buschmann, S.Lohmeier, and H.Ulbrich, "Humanoid robot Lola: Design and walking control," Journal of Physiology - Paris vol.103, pp.141-148, 2009.

[3] T.Buschmann, "Simulation and Control of Biped Walking Robots," PhD Thesis, Technischen Universität München, 2011.

[4] R.Tajima, D.Honda and K.Suga, "Fast Running Experiments Involving a Humanoid Robot," Proc. of IEEE Int. Conference on Robotics and Automation, pp.1571-1576, 2009.

[5] Y.Ogura, K.Shimomura, H.Kondo, A.Morishima, T.Okubo, S.Momoki, H.Lim, and A.Takanishi, "Human-like Walking with Knee Stretched Heel-contact and Toe-off Motion by a Humanoid Robot," Proc. of IEEE/RSJ Int. Conference on Intelligent Robots and Systems, pp.3976-3981, 2006.

[6] M-S.Kim, I.Kim, S.Park, and J-H.Oh, "Realization of Stretch-legged Walking of the Humanoid Robot," Proc. of IEEE-RAS Int. Conference on Humanoid Robots, pp.118-124, 2008.

[7] K.Hashimoto, Y.Takezaki, H.Motohashi, T.Otani, T.Kishi, H.Limi, and A.Takanishi, "Biped Walking Stabilization Based on Gait Analysis," Proc. of IEEE Int. Conference on Robotics and Automation, pp.154-159, 2012.

[8] K.Kaneko, F.Kanehiro et al., "Hardware Improvement of Cybernetic Human HRP-4C for Entertainment Use," Proc. of IEEE/RSJ Int. Conference on Intelligent Robots and Systems, pp.4392-4399, 2011.

[9] M.Vukobratović and B.Borovac, "Zero-Moment Point – Thirty File Years of Its Life –," International Journal of Humanoid Robotics, vol.1, no.1, pp.157-173, 2004.

[10] S. Kajita, M. Morisawa et al., "Biped Walking Stabilization Based on Linear Inverted Pendulum Tracking," Inter. Conf. on Intelligent Robots and Systems, pp.4489-4496, 2010.

[11] K. Miura, M. Morisawa et al., "Human-like Walking with Toe Supporting for Humanoids," Inter. Conf. on Intelligent Robots and Systems, pp.4428-4435, 2011.

[12] Kajita, S., Matsumoto, O. and Saigo, M., "Real-time 3D walking pattern generation for a biped robot with telescopic legs," Proc. of the 2001 ICRA, pp.2299-2306, 2001.

[13] Tomomichi Sugihara, "Standing Stabilizability and Stepping Maneuver in Planar Bipedalism based on the Best COM-ZMP Regulator," Proc. IEEE Int. Conference on Robotics and Automation, pp.1966-1971, 2009.

[14] Collins, S., Ruina, A., Tedrake, R. and Wisse, M., "Efficient Bipedal Robots Based on Passive-Dynamic Walkers," Science, Vol.307, pp.1082-1085, 2005.